



Late Pleistocene glacial history of Jameson Land, central East Greenland, derived from cosmogenic ^{10}Be and ^{26}Al exposure dating

LENA HÅKANSSON, HELENA ALEXANDERSON, CHRISTIAN HJORT, PER MÖLLER, JASON P. BRINER, ALA ALDAHAN AND GÖRAN POSSNERT



Håkansson, L., Alexanderson, H., Hjort, C., Möller, P., Briner, J. P., Aldahan, A. & Possnert, G.: Late Pleistocene glacial history of Jameson Land, central East Greenland, derived from cosmogenic ^{10}Be and ^{26}Al exposure dating. *Boreas*, Vol. 38, pp. 244–260. 10.1111/j.1502-3885.2008.00064.x. ISSN 0300-9483.

Previous work has presented contrasting views of the last glaciation on Jameson Land, central East Greenland, and still there is debate about whether the area was: (i) ice-free, (ii) covered with a local non-erosive ice cap(s), or (iii) overridden by the Greenland Ice Sheet during the Last Glacial Maximum (LGM). Here, we use cosmogenic exposure ages from erratics to reconcile these contrasting views. A total of 43 erratics resting on weathered sandstone and on sediment-covered surfaces were sampled from four areas on interior Jameson Land; they give ^{10}Be ages between 10.9 and 269.1 kyr. Eight erratics on weathered sandstone and till-covered surfaces cluster around ~70 kyr, whereas ^{10}Be ages from erratics on glaciofluvial landforms are substantially younger and range between 10.9 and 47.2 kyr. Deflation is thought to be an important process on the sediment-covered surfaces and the youngest exposure ages are suggested to result from exhumation. The older (>70 kyr) samples have discordant ^{26}Al and ^{10}Be data and are interpreted to have been deposited by the Greenland Ice Sheet several glacial cycles ago. The younger exposure ages (≤ 70 kyr) are interpreted to represent deposition by the ice sheet during the Late Saalian and by an advance from the local Liverpool Land ice cap in the Early Weichselian. The exposure ages younger than Saalian are explained by periods of shielding by non-erosive ice during the Weichselian glaciation. Our work supports previous studies in that the Saalian Ice Sheet advance was the last to deposit thick sediment sequences and western erratics on interior Jameson Land. However, instead of Jameson Land being ice-free throughout the Weichselian, we document that local ice with limited erosion potential covered and shielded large areas for substantial periods of the last glacial cycle.

Lena Håkansson (e-mail: lena.hakansson@geol.lu.se), Christian Hjort (e-mail: christian.hjort@geol.lu.se) and Per Möller (e-mail: per.möller@geol.lu.se), Department of Geology, Quaternary Sciences, GeoBiosphere Science Centre, Sölvegatan 12, SE-223 62 Lund, Sweden; Helena Alexanderson (e-mail: helena.alexanderson@umb.no), Norwegian University of Life Sciences, Department of Plant and Environmental Sciences, P.O. Box 5003, NO-1432 Ås, Norway; Jason Briner (e-mail: jbriner@buffalo.edu), Department of Geology, University at Buffalo, Buffalo, NY 14260, USA; Ala Aldahan (e-mail: ala.aldahan@geo.uu.se), Department of Earth Sciences, Villavägen 16, SE-752 36 Uppsala, Sweden; Göran Possnert (e-mail: goran.possnert@angstrom.uu.se), Tandem Laboratory, Uppsala University, SE-751 21 Uppsala, Sweden; received 14th March 2008, accepted 28th July 2008.

The Late Pleistocene glacial history of the Northeast Greenland continental margin has been reconstructed from decades of research (e.g. Washburn 1965; Lasca 1969; Funder 1972, 2004; Funder & Hjort 1973; Hjort 1979, 1981; Björck & Hjort 1984; Nam *et al.* 1995; Funder & Hansen 1996; Stein *et al.* 1996; Funder *et al.* 1998; Hansen *et al.* 1999). Much of the focus has been on the fjord area of Scoresby Sund and the Jameson Land Peninsula (Fig. 1), an area with an extensive Quaternary sediment record in a presently ice-free part of central East Greenland. Sugden (1974) described Jameson Land as an area with little or no sign of glacial erosion, mainly based on the highly weathered landscapes in the interior of the peninsula, and he proposed that the area had been covered by non-erosive ice during the Last Glacial Maximum (LGM). Funder (1989) suggested that lack of evidence of glacial erosion might rather be a result of long periods with ice-free conditions. The view of a restricted Greenland Ice Sheet advance during the LGM was supported by results of the Polar North Atlantic Margins (PONAM) project in the early 1990s. Then stratigraphic evidence was presented for deposition by the Greenland Ice Sheet on interior

Jameson Land during the Late Saalian in marine isotope stage (MIS) 6 (Funder *et al.* 1994, 1998; Möller *et al.* 1994). There is still debate, however, about whether the Greenland Ice Sheet only reached the inner continental shelf, leaving extensive coastal land areas free of ice (e.g. Funder 2004; Wilken & Mienert 2006), or whether it reached all the way onto the outer shelf or even to the shelf-break during the LGM (Evans *et al.* 2002; Ó Cofaigh *et al.* 2004).

In recent years, cosmogenic exposure dating methods have provided new techniques by which to interpret weathered landscapes differentially, and this has led to a new understanding of Pleistocene ice sheets elsewhere in the Arctic (Fabel *et al.* 2002; Stroeven *et al.* 2002; Briner *et al.* 2003, 2005, 2006; Landvik *et al.* 2003; Marquette *et al.* 2004; Davis *et al.* 2006; Harbour *et al.* 2006).

In the present study, we use cosmogenic exposure dating from 43 erratics (43 ^{10}Be ages and 5 ^{26}Al ages) to test whether the interior of Jameson Land was: (i) ice-free, (ii) covered with a local non-erosive ice cap(s), or (iii) overridden by the Greenland Ice Sheet during the LGM.

Geological setting

Scoresby Sund ($70\text{--}71^\circ\text{N}$, $22\text{--}28^\circ\text{W}$) is one of the major fjord systems in East Greenland (Fig. 1). The coastal areas beyond the present margin of the Greenland Ice Sheet in the Scoresby Sund region are dominated by three landscape types: (i) closest to the ice-sheet margin, deep fjords are cut into ice-covered high mountain plateaus of Caledonian crystalline bedrock, (ii) north of Scoresby Sund, on the Jameson Land Peninsula, Mesozoic sandstones and shales make up low-relief ice-free terrain, and (iii) south of Scoresby Sund, on the basaltic Geikie plateau, and east of Jameson Land, on the Caledonian crystalline terrain of Liverpool Land, the landscape has an alpine relief from local glaciation (Fig. 1).

The Jameson Land Peninsula has an asymmetric topographic profile. From the plateau areas of interior Jameson Land the terrain slopes gently towards Scoresby Sund in the west and south, whereas the eastern margin, facing Hurry Fjord, has a steeper gradient (Fig. 1). The plateaus form the watershed between east-draining rivers towards Hurry Fjord and the many, and commonly large, river valleys draining west and south towards Scoresby Sund.

Previous investigations

Two areas covered by Late Pleistocene glaciogenic sediments have been described on Jameson Land; the ‘older

drift’ and the ‘younger drift’ (Ronnert & Nyborg 1994). The former has been mapped on the upland plateaus on the interior of the peninsula (Möller *et al.* 1994), the latter on low elevation areas bordering Scoresby Sund (Ronnert & Nyborg 1994) (Fig. 1). Between these two regions is the so-called ‘drift-less area’, where weathered sandstone is exposed and glacial deposits only occur as scattered erratics and more rarely as thin patches of till (Hjort & Salvigsen 1991; Ronnert & Nyborg 1994).

The ‘older drift’

Already in the early parts of the 20th century, glacial and fluvial deposits were described on interior Jameson Land by Otto Nordenskjöld and referred to as the ‘Jameson Land Drift’ (Nordenskjöld 1907). It was suggested that these sediments were deposited during an extensive glaciation, first named the Kap Mackenzie stadial (Funder & Hjort 1973), later the Scoresby Sund glaciation (Funder 1984), and regarded to be early Weichselian or older in age. This chronology was based on the intense bedrock weathering of interfjord uplands along the northeast Greenland coast, and infinite ^{14}C dates from raised marine deposits north of Jameson Land were used to put minimum constraints on this glaciation (Funder & Hjort 1973; Hjort 1981). The ‘Jameson Land Drift’, later referred to as the ‘older drift’ (Ronnert & Nyborg 1994), is found as a continuous sheet

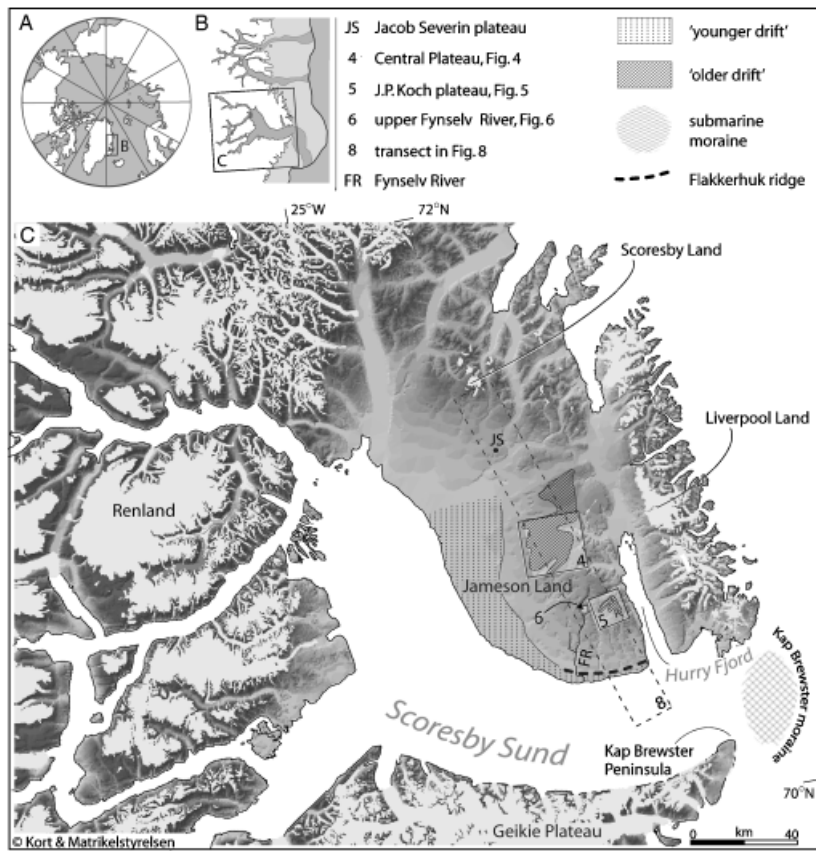


Fig. 1. A. The Arctic and the location of Greenland. B. Central East Greenland $\sim 68\text{--}74^\circ\text{N}$. The continental shelf is marked as a light grey area and cross-shelf troughs are shown in darker grey. C. The Scoresby Sund area and Jameson Land. Detailed site maps (Figs 4, 5, 6) are marked with framed boxes. The dashed frame shows the transect in Fig. 8.

on the Central Plateau at 450–500 m a.s.l. and on the J. P. Koch plateau at altitudes >750 m a.s.l. (Fig. 1). Erratics on weathered mountain plateaus on northern Jameson Land (e.g. Jacob Severin Bjerg) (Fig. 1) and discontinuous patches of till in the ‘drift-less’ area (e.g. the Fynselv area) have also been correlated with the ‘older drift’ (Möller *et al.* 1994).

Within the PONAM project, the stratigraphy of interior Jameson Land was investigated in river valleys at the edges of the Central Plateau (Möller *et al.* 1994). Successions of proglacial sediments and subglacial till were described and interpreted as having been deposited during two glacial advances in lakes dammed between the western edge of the Central Plateau and the margin of an advancing outlet glacier in Scoresby Sund. It was also suggested that till was deposited by the ice sheet successively overriding the plateau during the latter of the two advances. Five thermoluminescence (TL) ages constrain the deposition of till on the plateau to between 222 and 167 kyr, which indicates that the advance took place during the Late Saalian (Möller *et al.* 1994). Investigations at the eastern margin of the Central Plateau (Fig. 1) have shown that lakes were also dammed by a glacier advancing onto the plateau from Liverpool Land in the east during the Saalian (Möller *et al.* 1994; Adrielsson & Alexanderson 2005). The stratigraphy also reveals an ice advance from Liverpool Land during the Weichselian constrained by optically stimulated luminescence (OSL) ages from aeolian sediment giving it a maximum age of 109 kyr (Adrielsson & Alexanderson 2005).

The ‘younger drift’

Along the Scoresby Sund coast, the ‘younger drift’ extends to ~200 m a.s.l. (Fig. 1). Previous work has identified lacustrine and marine sediments and three thin and discontinuous till layers interpreted as three different advances of outlet glaciers in the Scoresby Sund during the Weichselian, reaching no further than the upper boundary of the ‘younger drift’. It was suggested that the two oldest advances of outlet glaciers occurred in the early Weichselian, during the Aucella and Jyllandselv stades (Landvik *et al.* 1994; Lyså & Landvik 1994; Tveranger *et al.* 1994; Funder *et al.* 1998) (Fig. 2). Hansen *et al.* (1999) interpreted part of the lacustrine sediments of the ‘younger drift’ as having been deposited in ice-dammed lakes adjacent to an outlet glacier advancing and retreating in Scoresby Sund during the last glaciation. OSL ages of the glaciolacustrine sediments constrain this last ice advance in the Scoresby Sund to between 60 and 10 kyr (Flakkerhuk stade). During the Late Weichselian, the northern margin of the outlet glacier was thought to be related to the Flakkerhuk ridge on southern Jameson Land (Fig. 1), which is an erosional landform composed of pre-LGM

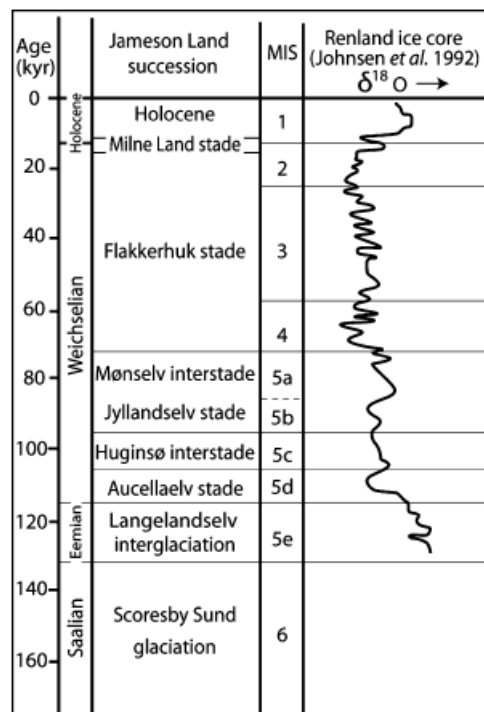


Fig. 2. The late Quaternary succession of Jameson Land and its proposed correlation with the European chronostratigraphy and the marine oxygen isotope stratigraphy, according to Funder *et al.* (1994). The correlation with the $\delta^{18}\text{O}$ record from the Renland ice core is also shown (Johnsen *et al.* 1992).

sediments (Tveranger *et al.* 1994). This would suggest that ice reached <70 m a.s.l. near Hurry Fjord during the LGM (Funder *et al.* 1998). The limited ice thickness near the fjord mouth was used to argue that the LGM ice terminated at the Kap Brewster submarine moraine (Dowdeswell *et al.* 1994) (Fig. 1), leaving Jameson Land above the ‘younger drift’ limit ice-free and the adjacent continental shelf free of grounded ice (e.g. Möller *et al.* 1994; Funder *et al.* 1998). An increased sediment input to the shelf break outside Scoresby Sund between 19 000 and 15 000 BP (Stein *et al.* 1993; Nam *et al.* 1995) was interpreted as the period when the ice front was standing at the Kap Brewster moraine (Dowdeswell *et al.* 1994). The oldest ^{14}C date from the sediments in Scoresby Sund is 10 200 BP and suggests a minimum age for the deglaciation of the outer fjord (Marienfeld 1991).

Methods

Samples for cosmogenic ^{10}Be and ^{26}Al dating were collected manually using hammer and chisel. Cobbles and pebbles were collected from flat, well-drained surfaces, and samples consist of either a single cobble or an amalgamated sample of ~15 clasts of about the same size (Table 1). Sample location and elevation were obtained using a GPS (global positioning system) receiver.

Table 1. Details of ^{10}Be and ^{26}Al analyses.

Sample	Surface type ^a	Sample height (m)	Lat. (N)	Long. (W)	Elevation (mas.l.)	Thickness correction ^b	Be carrier mass (mg)	Sample mass (g)	$^{10}\text{Be}/^{9}\text{Be}$ (ppm) ($\times 10^{12}$) ^c	$^{26}\text{Al}/^{27}\text{Al}$ ($\times 10^{12}$) ^d	^{10}Be age (kyr)	^{26}Al age (kyr)	$^{26}\text{Al}/^{10}\text{Be}$ ratio	
Jacob Severin Bjerg														
	Quartzite boulders													
CF-17	1a	0.4	71.123	23.290	444	0.983	0.359	40.051	126.7	0.945±0.049	1.183±0.078	70.2±9.2	67.2±9.7	6.4±0.9
CF-23	1a	0.6	71.123	23.285	445	0.983	0.359	40.161	113.6	0.894±0.055	1.178±0.085	66.0±9.0	59.7±8.8	6.1±0.9
CF-14	1a	0.4	71.123	23.285	446	0.983	0.356	24.967	n/a	0.59±0.032	69.5±9.2	n/a	n/a	n/a
	Cobbles (quartzite)													
CF-19	1b	n/a	71.123	23.285	445	0.944	0.321	40.273	n/a	1.057±0.065	n/a	72.7±7.6	n/a	n/a
CF-20	1b	n/a	71.122	23.285	445	0.921	0.359	40.302	n/a	0.726±0.093	n/a	54.5±9.7	n/a	n/a
The Central Plateau														
	Quartzite boulders													
UE-2	2a	0.3	70.542	23.154	446	0.983	0.349	39.846	n/a	2.465±0.088	n/a	183.8±23.8	n/a	n/a
UE-4	2a	0.5	70.544	23.215	410	0.983	0.347	40.298	n/a	1.791±0.055	n/a	134.3±17.0	n/a	n/a
	Crystalline boulders													
UE-19	2a	0.6	70.545	23.065	496	0.983	0.343	40.693	n/a	0.547±0.035	n/a	36.1±3.8	n/a	n/a
	Analgamated clast samples (crystalline)													
06-UE-3	2b	n/a	70.538	23.044	507	0.959	0.358	38.488	n/a	0.404±0.016	n/a	30.0±2.9	n/a	n/a
UE-6	2b	n/a	70.552	23.092	513	0.959	0.358	40.871	n/a	0.536±0.017	n/a	37.1±3.5	n/a	n/a
UE-7	2b	n/a	70.552	23.092	513	0.967	0.356	40.190	n/a	0.574±0.026	n/a	39.6±4.0	n/a	n/a
UE-10	2b	n/a	70.543	23.063	533	0.967	0.358	31.991	n/a	0.477±0.014	n/a	41.1±3.8	n/a	n/a
	Cobbles (crystalline)													
UE-9	2b	n/a	70.543	23.063	533	0.944	0.353	40.821	n/a	0.203±0.013	n/a	13.7±1.5	n/a	n/a
J.F. Koch Field														
	Quartzite boulders													
001	2a	0.4	70.39	22.46	782	0.983	0.348	40.048	n/a	0.633±0.054	n/a	33.2±4.9	n/a	n/a
004	2b	0.2	70.39	22.46	792	0.983	0.356	40.475	n/a	0.892±0.087	n/a	47.2±7.3	n/a	n/a
006	2b	0.3	70.39	22.46	782	0.983	0.357	40.037	n/a	0.3±0.05	n/a	16.1±3.3	n/a	n/a
008	2b	0.6	70.39	22.46	769	0.983	0.356	40.254	n/a	0.548±0.117	n/a	29.4±7.3	n/a	n/a
009	2b	0.4	70.39	22.46	770	0.983	0.357	46.613	n/a	0.235±0.08	n/a	10.9±3.9	n/a	n/a
	Crystalline boulders													
002	2a	0.1-0.3	70.39	22.46	775	0.983	0.356	27.344	n/a	0.583±0.059	n/a	46.3±7.3	n/a	n/a
011	2b	0.1-0.5	70.39	22.46	768	0.983	0.354	33.300	n/a	0.559±0.091	n/a	36.3±7.4	n/a	n/a
	Fynsely													
	Quartzite boulders													
FE-12	1a	0.3	70.363	23.151	338	0.983	0.354	39.172	74.1	1.989±0.103	3.696±0.216	169.1±17.9	141.0±20.7	5.5±0.8
FE-13	1a	0.6	70.361	23.163	318	0.983	0.356	40.640	81.9	1.547±0.097	2.691±0.190	129.0±14.3	114.2±17.2	5.8±0.7
FE-3	1a	0.1	70.345	23.175	257	0.983	0.358	40.345	n/a	2.185±0.072	n/a	199.0±19.5	n/a	n/a
FE-5	1a	0.15	70.345	23.164	257	0.983	0.357	40.667	n/a	2.036±0.097	n/a	182.8±19.1	n/a	n/a
FE-10	1a	0.6	70.364	23.144	353	0.983	0.357	40.667	n/a	3.170±0.148	n/a	269.1±28.4	n/a	n/a
FE-16	1a	0.4	70.322	23.163	235	0.983	0.357	40.544	n/a	1.111±0.056	n/a	100.1±10.3	n/a	n/a
FE-14	1a	0.4	70.352	23.162	323	0.983	0.358	40.075	94.1	1.323±0.084	2.074±0.138	111.3±12.3	99.9±14.7	6.0±0.6
06-FE-28	1b	0.7	70.392	23.105	487	0.983	0.356	40.051	n/a	1.520±0.041	n/a	108.7±10.2	n/a	n/a
06-FE-63	1a	0.35	70.373	23.076	442	0.983	0.358	40.640	n/a	3.311±0.077	n/a	253.9±24.4	n/a	n/a
06-FE-64	1a	0.3	70.374	23.076	442	0.983	0.360	40.075	n/a	2.949±0.074	n/a	229.3±22.0	n/a	n/a
06-FE-2	1b	0.3	70.383	23.080	493	0.983	0.331	24.967	n/a	1.456±0.042	n/a	156.3±14.9	n/a	n/a
06-FE-4	1b	0.2	70.385	23.082	495	0.983	0.357	24.950	n/a	1.767±0.128	n/a	207.1±24.7	n/a	n/a
06-FE-12	1b	0.25	70.385	23.071	531	0.983	0.544	39.397	n/a	1.298±0.032	n/a	139.4±13.0	n/a	n/a
06-FE-45	1b	0.3	70.383	23.081	525	0.983	0.356	40.067	n/a	1.157±0.037	n/a	79.2±7.5	n/a	n/a
06-FE-30	2a	0.5	70.386	23.069	485	0.983	0.335	40.161	n/a	1.042±0.031	n/a	69.5±6.5	n/a	n/a

Table 1. continued

Sample	Surface type ^a	Sample height (m)	Lat. (N)	Long. (W)	Elevation (mas.l.)	Thickness correction ^b	Be carrier mass (mg)	Sample mass (g)	Al (ppm)	¹⁰ Be/ ⁹ Be (×10 ¹²) ^c	²⁶ Al/ ²⁷ Al (×10 ¹²) ^d	¹⁰ Be age (kyr)	²⁶ Al age (kyr)	²⁶ Al/ ¹⁰ Be ratio
06-FE-40	2a	0.4	70.367	23.072	486	0.983	0.358	40.650	n/a	1.570±0.044	n/a	111.5±10.5	n/a	n/a
Crystalline boulders														
06-FE-59	2a	1.5	70.389	23.068	506	0.983	0.357	25.689	n/a	0.651±0.022	n/a	71.0±6.5	n/a	n/a
06-FE-60	2a	1.9	70.389	23.068	506	0.983	0.356	32.278	n/a	1.041±0.025	n/a	90.4±8.3	n/a	n/a
06-FE-69	2a	0.8	70.388	23.068	506	0.983	0.354	37.150	n/a	0.315±0.029	n/a	23.2±2.9	n/a	n/a
06-FE-62	2a	0.5	70.382	23.097	467	0.983	0.351	38.280	n/a	0.450±0.04	n/a	33.3±4.1	n/a	n/a
Amalgamated clast samples (quartzite and crystalline)														
06FFE-31	2a	n/a	70.3865	23.068	485	0.967	0.356	40.241	n/a	0.982±0.031	n/a	70.6±6.7	n/a	n/a
06FFE-32	2a	n/a	70.387	23.068	485	0.967	0.358	40.046	n/a	0.875±0.026	n/a	63.4±5.9	n/a	n/a
06FFE-61	2a	n/a	70.394	23.063	528	0.967	0.357	39.172	n/a	0.978±0.027	n/a	69.5±6.4	n/a	n/a

^aSurface type that the sample is resting on; (1a) regolith; (1b) weathered bedrock outcrops; (2a) flat till surface; (2b) glaciofluvial landforms.^bThickness correction calculated for a density of 2.68 g cm⁻³.^cBlank correction of 0.03076±0.00246×10⁻¹² applied. The ratio is normalized to NIST4325 (assuming an isotope ratio of 3.03×10⁻¹¹).^d¹⁰Be blank correction applied. The ratio is normalized to the standard of Nishiizumi (2004).

n/a not available or not applicable.

Shielding from surrounding objects was measured with a compass.

Samples were processed at the University at Buffalo for ¹⁰Be and ²⁶Al analysis following procedures modified after Kohl & Nishiizumi (1992) and Briner (2003). About 40 g of clean quartz from each sample was dissolved in batches of 11 and one process blank (Table 1). Known amounts of SPEX brand Be (~0.35 g) and Al carrier were added to all samples, including the blank. ¹⁰Be/⁹Be ratios were measured at the Tandem Laboratory at Uppsala University and normalized to the NIST SRM4325 standard (assuming an isotope ratio of 3.03×10⁻¹¹). ²⁶Al/²⁷Al ratios were measured at PRIME lab, Purdue University using the Al standard by Nishiizumi (2004). ¹⁰Be and ²⁶Al ages were calculated according to the scaling scheme for spallation by Lal (1991) and Stone (2000) using the CRONUS-Earth exposure age calculator version 2.2 available at <http://hess.ess.washington.edu/math/> (Balco *et al.* 2008). This version does an internal conversion of the ¹⁰Be data entered by the user to the revised ¹⁰Be standardization (isotopic ratio of the NIST SRM4325 standard is 2.79×10⁻¹¹) and ¹⁰Be half-life (1.36 Myr) of Nishiizumi *et al.* (2007). ¹⁰Be and ²⁶Al ages were calculated with reference production rates (2σ, sea level, high latitude and standard atmosphere) of 4.5±0.4 and 30.2±2.6 atoms/g/yr, respectively. Correction was made for sample thickness using exponential decrease in nuclide production and a bulk density of 2.68 g cm⁻³. The diameter of each cobble is used as its sample thickness, whereas the average diameter is used for amalgamated clast samples. The topographic shielding for all samples was less than 5° and was thus considered negligible. Snow shielding is also considered insignificant, since all samples were collected from exposed locations assumed to have been windswept during winters. The ¹⁰Be and ²⁶Al data are presented in Table 1.

The calculation of single cosmogenic exposure ages relies on several assumptions, including that a sampled surface has been constantly exposed, lacks inherited isotopes from previous exposures (requiring at least ~2 m of glacial erosion) (Davis *et al.* 1999; Briner *et al.* 2006), and has experienced only minimal postglacial surface erosion. This will likely be the case for most samples from erratics and bedrock surfaces from settings where substantial erosion took place. There are, however, at least two scenarios where these assumptions will be violated. First, exhumation of clasts from unconsolidated sediments will lead to anomalously young exposure ages (Putkonen & Swanson 2003). Second, non-erosive ice has the potential to preserve both old bedrock surfaces and erratics deposited during earlier glaciations, and thus samples from such surfaces might contain inherited isotopes from previous exposure, resulting in exposure ages much older than the last deglaciation (Briner *et al.* 2005).

Where bedrock and erratics are shielded from cosmic radiation for long periods (~200 kyr or longer; e.g. via

burial by non-erosive ice), the burial duration can be constrained using the disequilibrium of ^{10}Be and ^{26}Al concentrations (Lal 1991; Bierman *et al.* 1999; Gosse & Phillips 2001; Fabel *et al.* 2002; Briner *et al.* 2006; Harbour *et al.* 2006). In a continuously exposed surface ^{10}Be and ^{26}Al will be produced at a constant ratio of $^{26}\text{Al}/^{10}\text{Be} = 6.75 \pm 0.09$ (when using the revised ^{10}Be half-life) (Nishizumi *et al.* 2007). If a surface is shielded from cosmic radiation by non-erosive ice, then the faster decay of ^{26}Al (half-life of 700 kyr) relative to ^{10}Be (half-life of 1.36 Myr) will lead to a decrease in the $^{26}\text{Al}/^{10}\text{Be}$ ratio. Paired isotope data can thus constrain exposure and burial durations.

Results

Jakob Severin plateau – the ‘drift-less area’

The Jacob Severin plateau ($71^{\circ}12'\text{N}$, $23^{\circ}29'\text{W}$; Fig. 3A) is a sandstone plateau at ~ 450 m a.s.l. situated less than 30 km to the south from the mountainous Scoresby Land with present cirque glaciation at ~ 1000 m a.s.l. (Fig. 1). This plateau is covered by thin regolith com-

posed of sand and flat, sandstone cobbles. Along the plateau edges, weathered sandstone is exposed in small outcrops. Quartzite erratics occur scattered across the plateau and are suggested to be part of the ‘older drift’ (Möller *et al.* 1994).

Samples were taken from three wind-polished, 0.4–0.6 m high quartzite boulders resting on regolith (Fig. 3B) and two rounded quartzite cobbles perched on weathered bedrock outcrops (Table 1). ^{10}Be ages from boulders range between 66.0 ± 9.0 and 70.2 ± 9.2 kyr. Two of these samples (CF-17, 23) have $^{26}\text{Al}/^{10}\text{Be}$ ratios (within one sigma error) equivalent to the production ratio of 6.75 ± 0.09 . The two cobbles gave ^{10}Be ages of 54.5 ± 9.7 and 72.7 ± 7.6 kyr BP (Table 1). The ^{10}Be age of the youngest sample (CF-20) falls outside the two sigma range of the average age for the four oldest erratics. The average exposure age of the four oldest (\pm the standard deviation of the mean) is 68.8 ± 3.1 kyr.

The Central Plateau – the ‘older drift’

The Central Plateau ($\sim 70^{\circ}\text{N}$, 22°W ; Figs 1, 3C, 4) is situated ~ 40 km southeast of Jacob Severin Bjerg and



Fig. 3. A. The Jacob Severin plateau at ~ 450 m a.s.l. with Scoresby Sund in the background. B. Wind-polished quartzite erratic boulder on the Jacob Severin plateau (sample CF-17). C. The Central Plateau with the mountains of Liverpool Land in the background. The picture is taken from the plateau north of the Ugleelv valley. D. Section in glaciocluvial ridge on the eastern Central Plateau, south of the Ugleelv valley. The ridge is dominated by sandy sediments and on the surface there is a concentration of pebbles and cobbles. E. Esker on the J. P. Koch plateau, site JPK 1. Samples 008 and 009 are taken from the flat-topped mound seen in the background. F. Quartzite erratic boulder on the J. P. Koch plateau (sample 006) at site JPK 2. G. Sandstone tors in the Fynselv area. H. Crystalline erratic boulder on till in the Fynselv area (sample 06-FE-60).

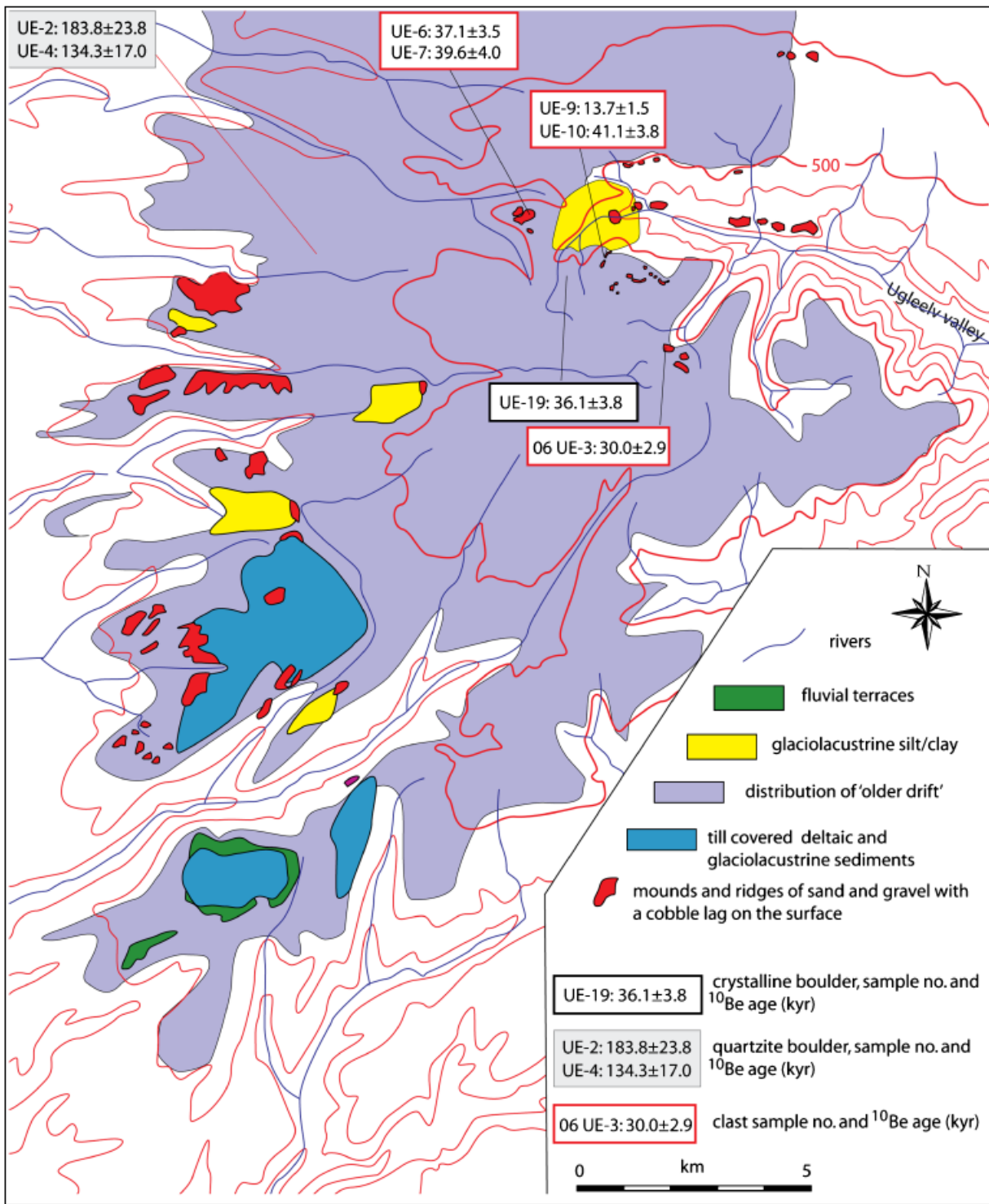


Fig. 4. Map of the Central Plateau based on Möller *et al.* (1994) and Adrielsson & Alexanderson (2005), combined with field mapping in 2006. Location of sampling sites and ^{10}Be ages are shown in inserted boxes.

constitutes an extensive flat area at 400–550 m a.s.l. This plateau is covered with thin sandy till (Möller *et al.* 1994) with a high abundance of wide-based erratic boulders, most of which reach <0.2 m above the till surface. Quartzites with a western provenance are the

most common boulder lithologies. Caledonian crystalline erratics, which have source areas to the west and on Liverpool Land to the east, are also present on the plateau. At around 400 m a.s.l., the western and southern parts of the plateau are incised by rivers discharging

into Scoresby Sund. Below this elevation the ‘older drift’ sediments become discontinuous with increased relief of the landscape (Fig. 4).

Along the margin of the Central Plateau there are several mounds and plateaus (up to 50 m high) and ridges (up to 10 m high) composed of unconsolidated sediments (Fig. 4). Large mounds and plateaus are found mostly along the western plateau margin and are interpreted as erosional remnants of the glaciolacustrine sediments deposited during the Saalian glaciation (Möller *et al.* 1994). Most of the considerably lower ridges are concentrated to the eastern plateau around the Ugleelv valley (Fig. 4). These landforms are composed of sand and gravel with some cobble-sized clasts and have been interpreted as glaciofluvial ridges deposited by an early Weichselian advance from the Liverpool Land ice cap into the valley (Adrielson & Alexanderson 2005). On the surfaces of these landforms there is a concentration of cobble-sized crystalline erratic material (Fig. 3D).

A total of eight samples were collected from boulders on the till plain and from clasts on the surfaces of glaciofluvial ridges around the Ugleelv valley (Fig. 4; Table 1). Two samples (UE-2, 4) were taken from 0.3–0.5 m high quartzite boulders on the western part of the plateau and these give ^{10}Be ages of 134.3 ± 17.0 and 183.8 ± 23.8 kyr (Table 1). One sample, collected from a 0.6 m high crystalline boulder on the eastern plateau margin adjacent to the Ugleelv valley (UE-19), has a ^{10}Be age of 36.1 ± 3.8 kyr. One cobble and four amalgamated clast samples were collected from the surfaces of

three ridges along the Ugleelv valley (Fig. 4). The cobble sample gives a ^{10}Be age of 13.7 ± 1.5 kyr and clast samples range between 30.0 ± 2.9 and 41.1 ± 3.8 kyr.

The J. P. Koch plateau – the ‘older drift’

J. P. Koch Fjeld is a basalt-capped mountain, reaching 909 m a.s.l. South and east of the mountain, Jurassic sandstone forms a flat plateau at 750–850 m a.s.l. (Fig. 5), covered by a thin till sheet and with weathered sandstone outcrops exposed along the plateau edges. Ridges and mounds are found near the plateau margin at sites JPK1, 2 and 3 (Fig. 3E) and terrace systems occur along the edges and on the upper slopes of the Harelv valley at site JPK4 (Fig. 5). The landforms are composed of sand and coarse-grained sediments with a maximum particle size of ~ 0.4 m and clasts are predominantly quartzite and crystalline erratics (Möller *et al.* 1994). There is a concentration of cobbles on the surface of these landforms and more rarely erratic boulders < 0.6 m. Boulder-sized erratics are common on the thin drift sheet covering the plateau. These landforms were interpreted as eskers and kames (Möller *et al.* 1994). Three TL ages from sites JPK1–3 range between 167 and 380 kyr (Fig. 5) and, based on these ages and the content of western quartzite boulders, it has been suggested that they were deposited by the Greenland Ice Sheet during the Saalian glaciation (Möller *et al.* 1994).

A total of seven samples were collected from boulders resting on drift on the J. P. Koch plateau (Table 1,

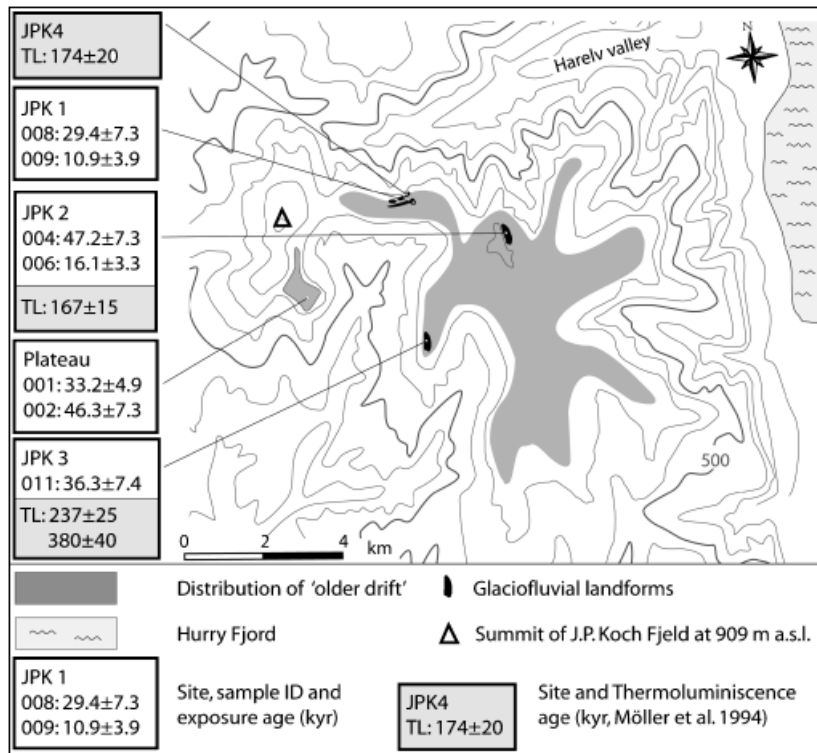


Fig. 5. Map of the J. P. Koch plateau after Möller *et al.* (1994) showing drift distribution and location of glaciofluvial landforms. Our ^{10}Be results are shown together with TL ages from Möller *et al.* (1994).

Fig. 5). Two samples are from quartzite boulders on the surface of the glaciofluvial mound at site JPK1 (Fig. 3E), one of them from a 0.4 m high boulder resting on the flat crest far away from the slopes (sample 009), the other a 0.6 m high boulder resting on a gently sloping surface slightly below the crest (sample 008). Two samples were taken from 0.2 and 0.3 m high quartzite boulders (samples 004 and 006, respectively), resting on a gently sloping surface just below the crest of the glaciofluvial ridge at site JPK2. One crystalline boulder was sampled from the crest of the glaciofluvial ridge at site JPK3 (sample 011). Samples were also collected from the till-covered plateau south of the summit of J. P. Koch Fjeld, from one quartzite (sample 001) and one crystalline boulder (sample 002).

The ages form two groups, one slightly younger than the other, but both groups are substantially younger than TL ages from sediment samples in this area (Fig. 5) (Möller *et al.* 1994). Samples 006 and 009 give ^{10}Be ages of 16.1 ± 3.3 and 10.9 ± 3.9 kyr, whereas the remaining five samples range between 29.4 ± 7.3 and 47.2 ± 7.3 kyr (Table 1).

The Fynselv area – the ‘drift-less’ area’

The Fynselv River has its source northwest of the J. P. Koch plateau and discharges to the south into Scoresby

Sund (Fig. 1). The upper and middle reaches of this river flow through the ‘drift-less’ area, and it has formed deep canyons surrounded by extensive interfluves of exposed weathered sandstone between ~ 550 and 250 m a.s.l. The centre of interfluves is covered by regolith. Along the edges of the canyon, tors-rich areas are common (Fig. 3F), and in some areas systems of meltwater channels follow fracture systems in the sandstone (Schunke 1986; Hjort & Salvigsen 1991; Håkansson 2008) (Fig. 6).

In the Fynselv area, drift cover is rare and occurs only as patches of sandy till and single erratics, usually on regolith-covered centres of interfluves but also on weathered sandstone outcrops within tors areas. The drift cover is dominated by rounded quartzite cobbles and wind-polished quartzite boulders <0.6 m high. Large (up to 2 m high) and angular crystalline erratics occur scattered on till-covered surfaces (Fig. 3G).

Twenty-three samples were collected from boulders and clasts resting on both till and weathered bedrock (Table 1). Most samples (sample ID starting with 06-) were taken from one area at the upper reaches of the river ($\sim 70^{\circ}38'\text{N}$, $23^{\circ}07'\text{W}$) (Figs 1, 6). The remaining samples were collected from areas further to the south, downstream along the Fynselv River, and all are from regolith-covered surfaces on the centre of interfluves.

In total, 14 samples from wind-polished quartzite erratics, 0.1–0.6 m high, were collected from weathered

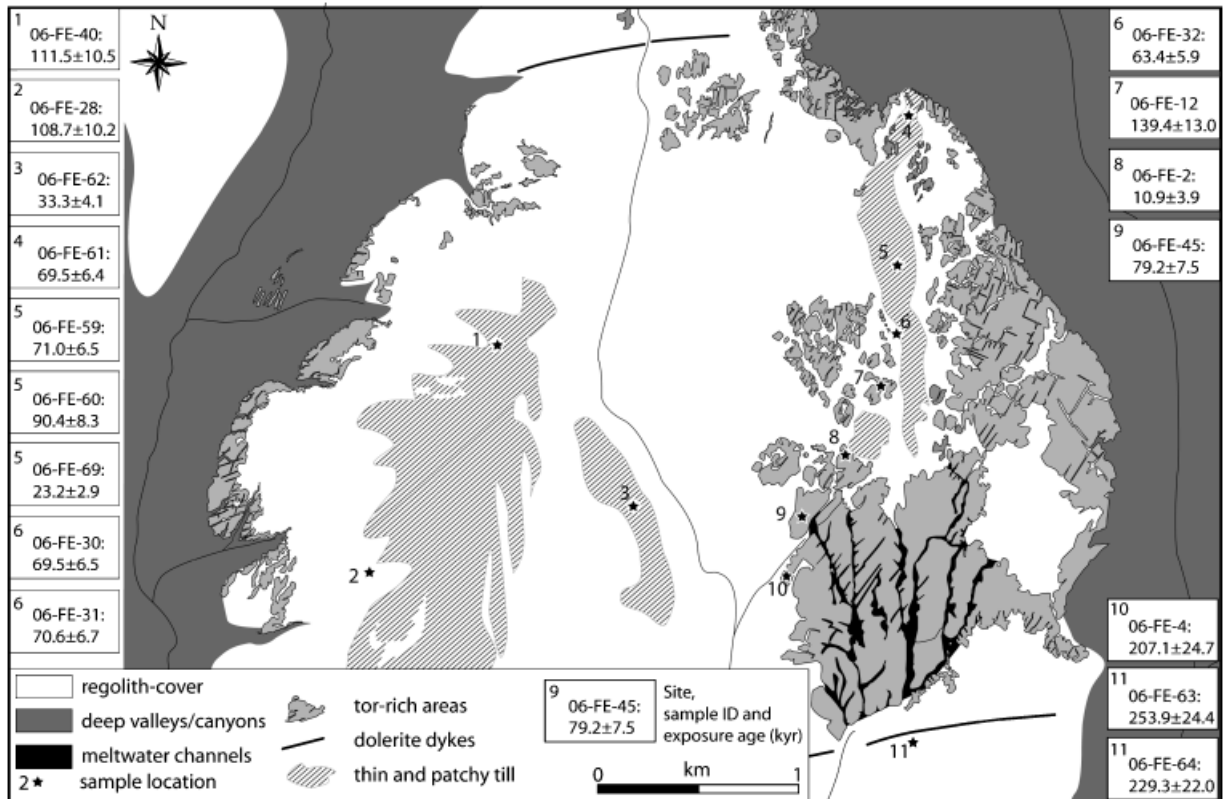


Fig. 6. The tors area at the upper reaches of the Fynselv River (where samples with the prefix 06- were collected). The distribution of drift-cover and tors-rich areas is shown. The locations of samples are marked with stars and ^{10}Be ages (Table 1) are shown in framed boxes.

bedrock surfaces or surfaces covered by regolith. Acquired ^{10}Be ages for these boulders are scattered between 79.2 ± 7.5 and 269.1 ± 28.4 kyr. ^{26}Al has been measured on three samples (FE-12, 13, 14), all with $^{26}\text{Al}/^{10}\text{Be}$ ratios discordant to the production ratio of 6.75 ± 0.09 (Table 1). Samples were also collected from erratics on the thin patches of till along the upper reaches of the river (Fig. 6); three clast samples (06FE-31, 32, 61) give ^{10}Be ages between 63.4 ± 5.9 and 70.6 ± 6.7 kyr, four samples from crystalline boulders 0.4–1.9 m high range between 23.2 ± 2.9 and 90.4 ± 8.3 kyr and two quartzite boulders (06FE-30, 40) 0.4 and 0.5 m give ^{10}Be ages of 69.5 ± 6.5 and 111.5 ± 10.5 kyr.

The larger part of the data set from the Fynselv area shows a scattered distribution of ^{10}Be ages that range from 23.2 ± 2.9 to 269.1 ± 28.4 kyr, but five samples (06FE-30, 31, 32, 59, 61) form a cluster with an average age of 68.8 ± 3.1 kyr.

Summary of exposure ages

^{10}Be exposure ages of erratics from interior Jameson Land have been divided into two groups based on whether sampled erratics were resting on weathered sandstone (Fig. 7A) or on sediment (Fig. 7B). Erratics on weathered sandstone surfaces in the Fynselv area have ‘old’ exposure ages, with a scattered distribution between ~ 80 and 270 kyr. However, there are also a few ‘old’ samples from sediment-covered surfaces (Fig. 7B); two are from the Fynselv area (samples 06FE-40, 60) and two from the till plain on the western Central Plateau (samples UE-2, 4). The younger part of the data

set, with ^{10}Be exposure ages between ~ 11 and 71 kyr, is distributed over both weathered sandstone and sediment-covered surfaces. The youngest erratics on weathered sandstone surfaces are from the Jacob Severin plateau and cluster around ~ 70 kyr, which is similar to ages of erratics from till in the Fynselv area. The exposure ages from both the J. P. Koch plateau and the eastern Central Plateau are younger compared to the rest of the data set (Fig. 7), but also considerably younger than the age proposed by earlier work for glaciofluvial landforms on these plateaus (Möller *et al.* 1994; Adriaelsson & Alexanderson 2005) (Fig. 5). On sediment-covered surfaces (till plains and glaciofluvial landforms), samples cluster around the oldest ages, and in this population a few young outliers are found (Fig. 7). In the present study, three samples give ^{10}Be exposure ages compatible with a LGM deglaciation. All of these are from glaciofluvial landforms; one (sample UE-9) is taken from a ridge on the Central Plateau deposited by an advance of the Liverpool Land ice cap (Adriaelsson & Alexanderson 2005) and two (samples 006 and 009) are from ridges on the J. P. Koch plateau interpreted by earlier work to have been deposited by the Greenland Ice Sheet (Möller *et al.* 1994).

Discussion

The majority of the ‘old’ erratics in the Fynselv area are situated on sandstone surfaces adjacent to or on well-developed tors. Discordant paired isotope data from three of these erratics (samples FE-12, 13, 14) indicate a complex exposure/burial history longer than ~ 200 kyr, probably due to periods of shielding by ice with limited

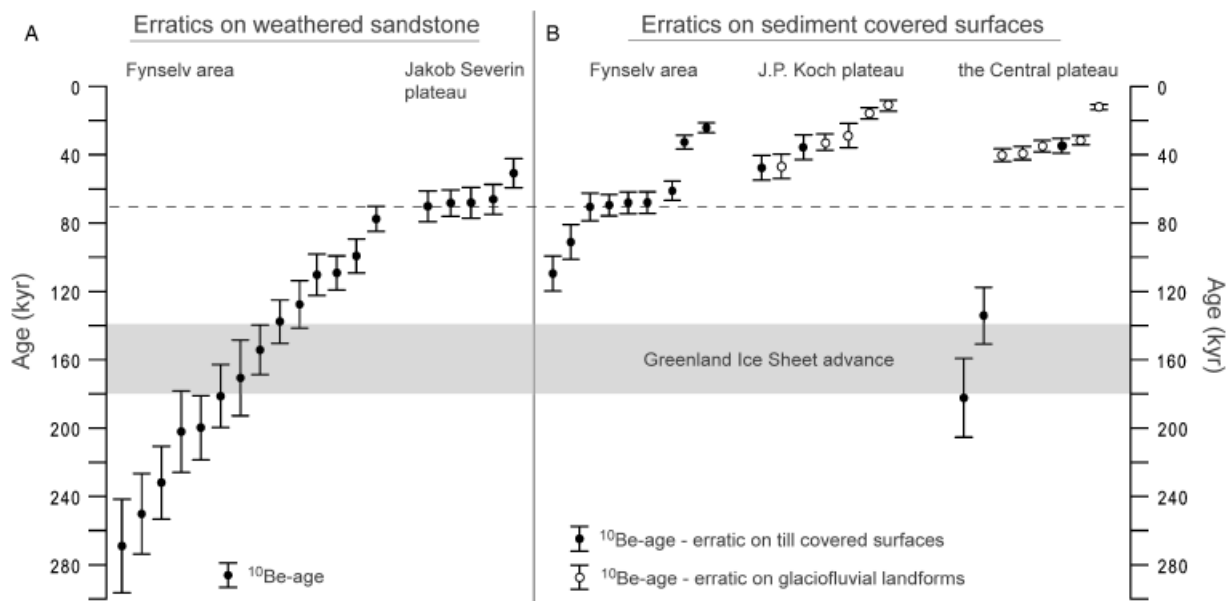


Fig. 7. All ^{10}Be ages on erratics from interior Jameson Land presented within two sigma error (Table 1). A, B. The distribution of ^{10}Be ages from erratics resting on weathered sandstone (A) and sediment-covered surfaces (B). Shading indicates the timing of the Saalian advance of the Greenland Ice Sheet (Funder *et al.* 1994). The dashed line marks the clustering of exposure ages around 70 kyr.

erosion potential. This suggests that both erratics and tors may have been preserved beneath ice with limited erosion potential. The total exposure and burial duration of a sample can be estimated based on measured ^{26}Al and ^{10}Be concentrations, assuming that the sampled surface only experienced one single burial event (Bierman *et al.* 1999). Consequently, paired isotope data can only provide a minimum estimate of the exposure/burial history. ^{26}Al and ^{10}Be concentrations presented here (from samples FE-12, 13, 14) indicate that at least some ‘old’ erratics in the Fynselv area were eroded from their source areas west of Jameson Land ~ 250 – 400 kyr ago (corresponding to MIS 8–12). Either these erratics were originally deposited on Jameson Land or they were entrained by a later advance of the ice sheet and successively brought to their present locations.

The younger part of the data set (^{10}Be exposure ages between ~ 11 and 71 kyr) can be interpreted in at least three ways, representing alternative scenarios for the timing of the last ice-sheet advance onto interior Jameson Land. The three different scenarios suggest that the last time Jameson Land was covered by the Greenland Ice Sheet was during: (i) the Saalian glaciation, (ii) the early Flakkerhuk stade (MIS 4), or (iii) the LGM.

(i) Previous work based on the stratigraphic record on Jameson Land suggests that the last time material was transported by the Greenland Ice Sheet onto the interior of the peninsula was during the Saalian glaciation (Möller *et al.* 1994). The exposure ages presented in this study, however, are much younger than the Saalian deglaciation (the transition between MIS 6 and 5e ~ 130 kyr BP).

(ii) In the stratigraphy of the ‘younger drift’ there is evidence of an advance of an outlet glacier in Scoresby Sund starting around ~ 70 kyr ago (Hansen *et al.* 1999), which corresponds with the clustering of our exposure ages around the same time.

(iii) Results from previous work based on exposure dating have indeed indicated the presence of non-erosive ice on interior Jameson Land during the LGM, but it has not been possible to conclude whether or not this ice was dynamically connected to the Greenland Ice Sheet (Håkansson *et al.* 2007; Håkansson 2008). In the present study, three samples give ^{10}Be exposure ages compatible with a LGM deglaciation.

The young samples mentioned in scenario (iii) are all taken from the surfaces of glaciofluvial ridges. The ages of the sampled landforms on the J. P. Koch and Central plateaus have been independently constrained with TL and OSL ages indicating deposition during the Saalian and the Early Weichselian, respectively (Möller *et al.* 1994; Adriaansson & Alexanderson 2005). Recent investigations have suggested that, when using cosmogenic exposure dating on old (pre-LGM) landforms, it is important to consider surface lowering processes causing exhumation (Putkonen & O’Neil 2006; Briner

2007; Kaplan *et al.* 2007). Cobbles and boulders on our sampled glaciofluvial landforms have similar maximum particle size and clast lithologies as the sediment found within these features. The clast concentrations on the surfaces of these landforms might thus be interpreted as a result of exhumation rather than deposition by an ice sheet during the LGM. This interpretation is further supported by the contrast between young exposure ages and much older TL and OSL ages of the landforms. In line with this reasoning, we find that a LGM advance of the Greenland Ice Sheet onto interior Jameson Land is unlikely.

Marine cores from the shelf break outside Scoresby Sund show lower sedimentation rates during MIS 4 compared to all other periods during the last glacial cycle (Nam *et al.* 1995). Additionally, there are no indications in the terrestrial stratigraphic record that the advance described in scenario (ii) was extensive enough to reach onto interior Jameson Land. These arguments are used against a large-scale advance of the Greenland Ice Sheet during MIS 4. Instead, we suggest that the erratics were deposited during the Saalian glaciation described in scenario (i). The exposure ages younger than the Saalian deglaciation are interpreted as a result of periods of shielding by non-erosive local ice cap(s) during the Weichselian. It is possible to calculate the thickness of ice required to inhibit production of ^{10}Be and ^{26}Al in a rock surface. For ^{10}Be concentrations to remain at or below the AMS detection limit ($\sim 20\,000$ atoms), ice would need to be at least 30 m thick at 500 m a.s.l. and at least 40 m at 800 m a.s.l. (calculated using an ice density of 0.92 g cm^{-3} and the production proportions of ^{10}Be and ^{26}Al described in the methods chapter). These thicknesses will inhibit spallogenic production, but will allow some muogenic production to take place in the glacial substrate. However, muogenic production rates are low (accounting for $<5\%$ of the production of ^{10}Be and ^{26}Al) (Helsinger *et al.* 2002), and to allow accumulation of significant ^{10}Be and ^{26}Al concentrations, ice would have to remain at these thicknesses for long intervals (throughout several glacial cycles). Thus, muon production can be considered negligible for the younger part of our data set (^{10}Be exposure ages between ~ 11 and 71 kyr) and therefore ice must have been at least 40 m thick on the J. P. Koch plateau and at least 30 m thick at 500 m a.s.l. in the Fynselv area, on the Jacob Severin and Central plateaus, to inhibit production of ^{10}Be and ^{26}Al in the underlying rock. In the glaciation model described below, we use these ice thicknesses to calculate the duration of periods of exposure and shielding by non-erosive local ice cap(s) on interior Jameson Land during the last ~ 130 kyr BP, that is since the Saalian deglaciation. However, when ice thins below these thicknesses, production will increase rapidly. Thus, the proposed exposure durations presented below are only minimum estimates.

A glaciation model of the Late Pleistocene on Jameson Land

Exposure and burial history of interior Jameson Land during the past \sim 130 kyr

Based on the younger part of our data set (^{10}Be exposure ages between \sim 11 and 71 kyr), we suggest that the Jacob Severin plateau and the Fynselv area were exposed for a total of \sim 70 kyr and completely shielded by ice for \sim 60 kyr. The J. P. Koch plateau, situated on elevations \sim 300 m higher compared to the other areas, would have been exposed for \sim 50 kyr according to the oldest exposure ages at this site and therefore covered for \sim 80 kyr. These periods of shielding are too short to be resolved by paired ^{10}Be and ^{26}Al data and accordingly samples from the Jacob Severin plateau (CF-17, 23) give $^{26}\text{Al}/^{10}\text{Be}$ ratios indicating ‘constant exposure’. On the eastern Central Plateau the oldest samples suggest a minimum exposure period of \sim 40 kyr. The duration of shielding, however, will depend on the timing of the early Weichselian advance from the Liverpool Land ice cap, which deposited the sampled landforms. This advance is constrained by three OSL dates of aeolian sediment (a maximum of 109 kyr and two minimum ages of 27 and 10 kyr) and is thought to have taken place during the Early Weichselian, either in MIS 5d or MIS 5b (Adrielson & Alexanderson 2005).

Glaciological conditions

The Renland ice core indicates that during the MIS 5e the snow accumulation rate in the Renland ice cap was 20% higher than at present (Johnsen *et al.* 1992) (Figs 1, 2). Such high accumulation during the transition from interglacial to glacial climate would favour growth of local ice caps on high-elevation regions such as the two presently glaciated areas to the north and east of Jameson Land (Fig. 1), the Scoresby Land mountains (\sim 1000 m a.s.l.) and Liverpool Land (highest peak is \sim 1400 m a.s.l.), but also on the J. P. Koch plateau (\sim 800 m a.s.l.). The Scoresby Land and Liverpool Land mountains were most likely glaciated throughout the last glacial cycle. Out of the three accumulation centres mentioned above, Liverpool Land is most heavily glaciated at present and due to its coastal location it would probably have received more precipitation all through the last glacial cycle compared to the other areas. The J. P. Koch plateau is situated on lower elevations compared to the other two areas and in addition its location further away from the coast will also result in less precipitation than on Liverpool Land.

Sequential model

Based on the ^{10}Be and ^{26}Al exposure age data set in combination with the stratigraphical record (e.g.

Funder *et al.* 1994, 1998; Möller *et al.* 1994) and the climate record from the Renland ice core (Fig. 2) (Johnsen *et al.* 1992), a sequential model of Late Pleistocene events in the Jameson Land area is proposed in 11 steps (Fig. 8A–K). The four investigated areas are shown along an approximated transect from the Scoresby Land mountains in the NW to the Scoresby Sund trough in the SE (Figs 1, 8).

A. Erratics with ‘old’ exposure ages, as seen in the Fynselv area and from the western Central Plateau, were originally deposited on Jameson Land or adjacent areas between \sim 250 and 400 kyr ago by the Greenland Ice Sheet (Fig. 8A).

B. During the Saalian glaciation an advance of the Greenland Ice Sheet deposited erratics on the Jacob Severin plateau and in the Fynselv area. Also, some pre-Saalian quartzite boulders (samples UE-2, 4; see Table 1) were redeposited in the Saalian till on the Central Plateau. This till was at least partly deposited by active warm-based ice (Möller *et al.* 1994), whereas tors in the Fynselv were preserved beneath ice with limited erosional properties (Håkansson 2008) (Fig. 8B). The ice-sheet margin probably reached the continental shelf break at this time. During deglaciation, glaciofluvial ridges were formed along the edges of the J. P. Koch plateau (Möller *et al.* 1994). Meltwater incised the Central Plateau and formed the Ugleelv valley (Adrielson & Alexanderson 2005).

C. The marine limit following the Saalian deglaciation was \sim 70 m a.s.l. at the middle reaches of the fjord (Landvik *et al.* 1994). Summer temperatures on Jameson Land were \sim 5°C warmer than at present during the Langelandselv interglacial (MIS 5e, the Eemian) (Bennike & Böcher 1994) and with \sim 20% more precipitation (Johnsen *et al.* 1992). Possible exposure time for surficial boulders during this ice-free interval was \sim 15 kyr (Fig. 8C).

D. Either during the last part of the Langelandselv interglacial or in the initial phase of the Weichselian glacial cycle, in the Aucella stade (MIS 5d), high precipitation and cooling temperatures led to growth of local ice caps on major accumulation centres such as the Scoresby Land mountains, Liverpool Land and the J. P. Koch plateau (Fig. 8D). Temperatures were 5–10°C colder than present (Funder *et al.* 1998). A westward advance from the Liverpool Land ice cap might have reached into the Ugleelv valley. At around the same time, an outlet glacier from the Greenland Ice Sheet expanded in the Scoresby Sund trough and deposited a till as part of the ‘younger drift’ along the Jameson Land coast (Funder *et al.* 1998) (Fig. 1). The Jacob Severin plateau and the Fynselv area remained ice-free throughout this period lasting for \sim 10 kyr.

E. During the Huginsø interstadie (MIS 5c), the precipitation was \sim 30% of the present (Johnsen *et al.* 1992) and maximum summer temperatures nearly reached present values (Funder *et al.* 1998). Hence the local ice cap

on the J. P. Koch plateau melted away and ice centred on the Scoresby Land mountains and on Liverpool Land retreated, resulting in ice-free conditions on interior Jameson Land. The exposure periods on the Jacob Severin plateau and in Fynselv probably lasted ~ 15 kyr and slightly less on the J. P. Koch plateau (Fig. 8E).

F. Temperatures dropped during the Jyllandselv stade (MIS 5b) to 5–10°C colder than present, but pre-

cipitation was still $\sim 30\%$ of the present. Again, local ice started to build up over the J. P. Koch plateau, but this time it also covered the Fynselv area (Fig. 8F). Ice on the accumulation centre in the Scoresby Land mountains expanded to the Jacob Severin plateau. At all three sites, ice must have been non-erosive to allow the preservation of delicate landforms (glaciofluvial ridges, tors and weathering mantles). At around the

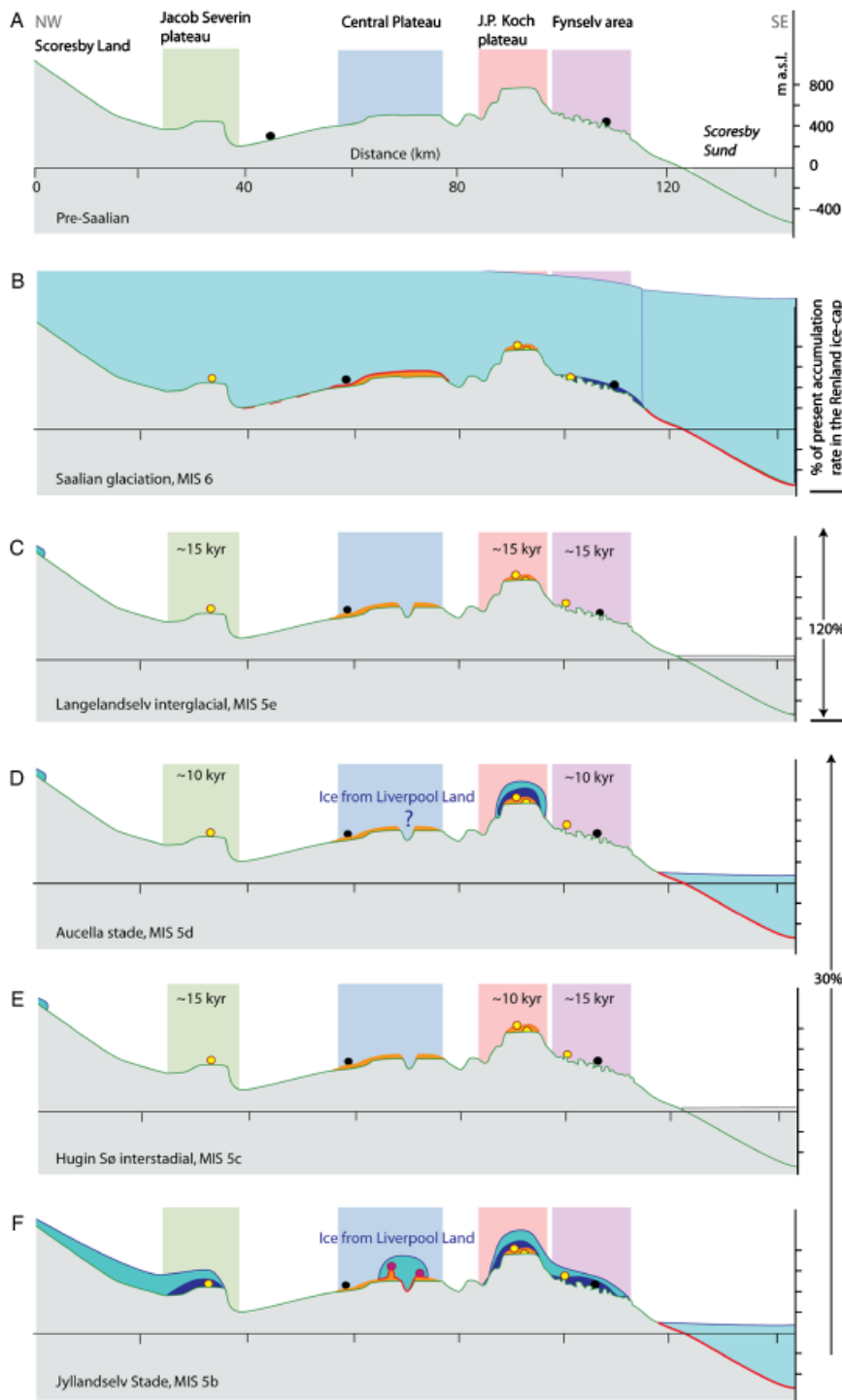


Fig. 8. Simplified model showing one possible scenario for the Late Pleistocene glacial geological development of interior Jameson Land. The accumulation rate in the Renland ice cap is shown in the right margin and is presented as percentage of present values.

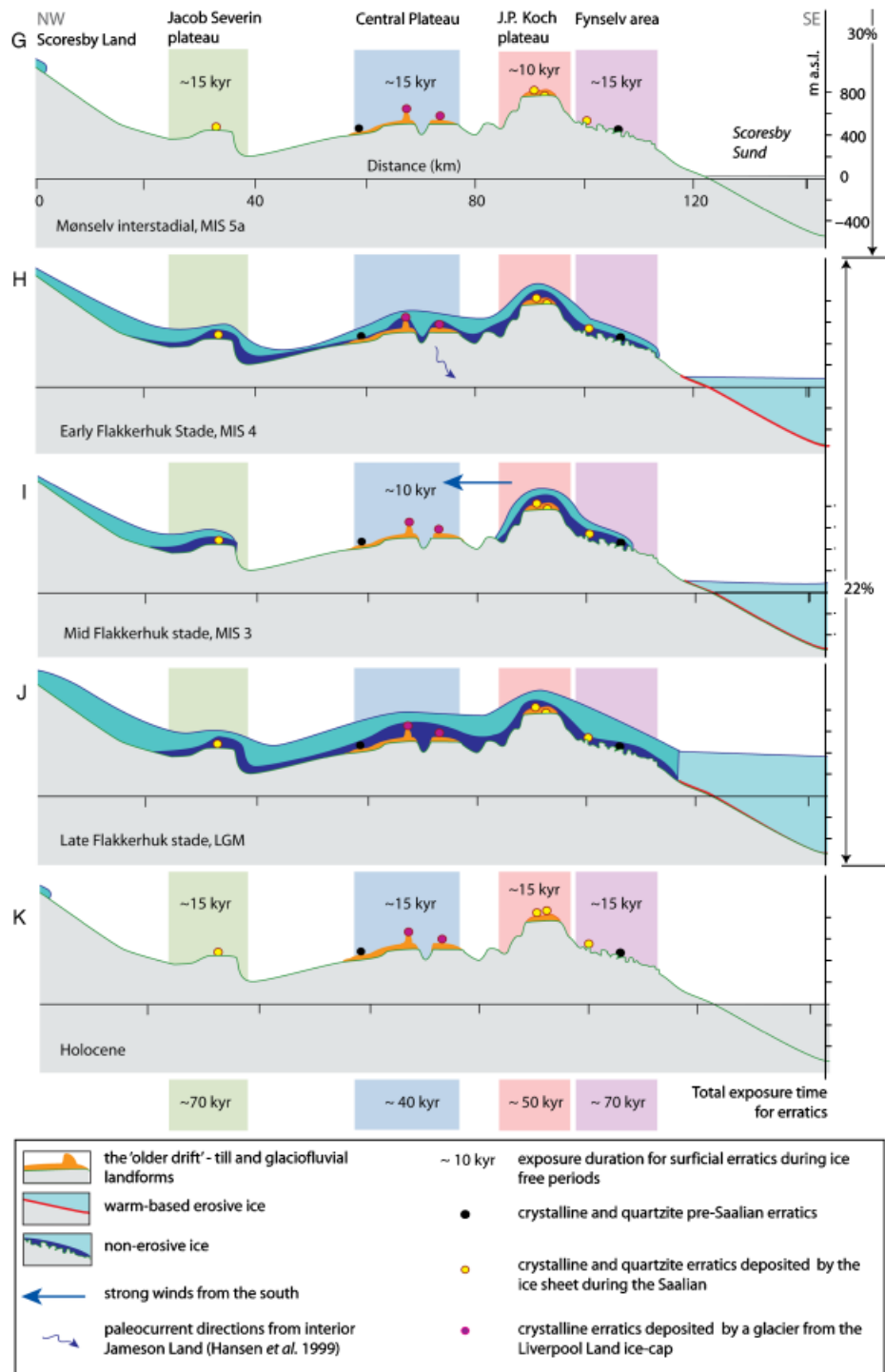


Fig. 8. Continued.

same time there was an active westward advance of a glacier from Liverpool Land, this time depositing till in the Ugleelv valley and glaciofluvial landforms on the edge of the Central Plateau adjacent to this valley (Adrielson & Alexanderson 2005). An outlet glacier advanced in the Scoresby Sund trough and deposited till within the 'younger drift' zone (Funder *et al.* 1998).

G. Once again, maximum summer temperatures nearly reached present values during the Mønselv interstadial (MIS 5a), but the precipitations stayed unchanged. This period lasted slightly longer than MIS 5c (Fig. 2; Johnsen *et al.* 1992). Local ice on interior Jameson Land melted away, resulting in an ice-free period of around 15 kyr in all areas except the J. P. Koch plateau, where ice lingered slightly longer,

resulting in ~10 kyr of exposure (Fig. 8G). Also during this period, strong winds might have eroded drift surfaces.

H. During the early Flakkerhuk stade (MIS 4) the climate got 10–20°C colder than present (Funder *et al.* 1998) and drier with only 22% of the present precipitation (Johnsen *et al.* 1992). This prolonged cold period led to slow accumulation of local ice over all plateaus, eventually coalescing into a thin, probably non-erosive, ice capping interior Jameson Land. Again, an outlet glacier advanced in the Scoresby Sund trough. Deltaic sediments were deposited in glacial lakes in marginal positions to the Scoresby Sund-based outlet glacier, and palaeoflow directions were from Scoresby Sund but also from interior Jameson Land (Hansen *et al.* 1999), probably caused by surface melt of the local ice cap during summers (Fig. 8H).

I. During the mid-Flakkerhuk stade (MIS 3), temperatures got slightly warmer compared to MIS 4, but the precipitation was unchanged (Johnsen *et al.* 1992). This resulted in ice starvation and melting/evaporation on the Central Plateau. An ice-free period lasting for ~10 kyr followed, when strong winds from the south formed deflation surfaces on the drift and accumulated sand dunes in the upper Ugleelv valley (Adrielson & Alexanderson 2005) (Fig. 8I). In contrast, ice could linger on the J. P. Koch plateau and in the Fynselv area, where some precipitation was brought by the southerly winds. The ice cover on the Jacob Severin plateau also persisted through this period because of its proximity to the Scoresby Land mountains. Prior to the LGM, ice probably accumulated again on the Central Plateau.

J. During the LGM, the local ice cap(s) coalesced with active ice in the Scoresby Sund trough (Fig. 8J). The probably non-erosive ice capping interior Jameson Land buttressed active ice in the fjord trough, allowing it to reach at least 250 m above the present sea level at the mouth of the Scoresby Sund fjord (Håkansson *et al.* 2007). At this time the ice margin probably reached a considerable distance onto the continental shelf. Ice on the tors area along the Fynselv River started to melt at the earliest around ~17 kyr ago (Håkansson 2008). The upper part of the Kap Brewster peninsula was deglaciated between 15 and 17 kyr BP (Håkansson *et al.* 2007), and the ice had totally left the outer fjord area before 10.2 kyr BP (Marienfeld 1991).

K. Following the deglaciation of interior Jameson Land the youngest erratics were gradually exhumed and exposed on the drift-covered plateaus. The total postglacial exposure time of interior Jameson Land until the present is suggested to have been about 15 kyr. When adding the duration of all ice-free periods in the presented model, the total exposure of the Jacob Severin plateau and Fynselv is ~70 kyr, on the J. P. Koch plateau ~50 kyr and on the Central Plateau ~40 kyr (Fig. 7K).

Conclusions

Our ^{10}Be and ^{26}Al exposure ages of erratics from four areas on interior Jameson Land can be divided into three groups: (i) ‘old’ erratics with total exposure and burial histories of ~250–400 kyr, estimated from discordant ^{10}Be and ^{26}Al data, (ii) ^{10}Be ages of erratics on weathered bedrock and till-covered surfaces clustering around ~70 kyr, and (iii) exposure ages from erratics on glaciofluvial ridges and till-covered plateaus ranging between 10.9 and 47.2 kyr. The ‘old’ exposure ages are interpreted to represent erratics deposited by the Greenland Ice Sheet several glacial cycles ago. Erratics with exposure ages \leq 70 kyr are suggested to originate from an ice-sheet advance during the Saalian glaciation and an advance by the local Liverpool Land ice cap during the Early Weichselian. The fact that the apparent exposure ages are younger than both the Saalian and the Early Weichselian is explained by the erratics, following deposition, being shielded from cosmic radiation during periods when substantial areas on Jameson Land were covered by non-erosive ice. The LGM/Lateglacial exposure ages from the top surfaces of glaciofluvial ridges are interpreted as results of exhumation; we suggest that the Greenland Ice Sheet did not cover Jameson Land during the LGM. Instead, we believe that, during this time and also during substantial periods of the last (Weichselian) glacial cycle, the area was covered by local ice cap(s) with limited erosion potential.

Acknowledgements. – This research was funded by the Helge Ax:son Johnson Foundation, the Swedish Association for Anthropology and Geography (SSAG) and Kungliga Fysiografiska Sällskapet in Lund. The Danish Polar Centre provided logistic support. Elizabeth Thomas is acknowledged for enthusiastic help and great company in the field and Nicolas Young is thanked for assistance in the laboratory. Nicolaj Krog Larsen and Lena Adrielson are acknowledged for valuable discussions on this manuscript. Particular thanks to Jon Landvik and Vincent Rinterknecht for constructive and helpful reviews of our paper.

References

- Adrielson, L. & Alexanderson, H. 2005: Interactions between the Greenland Ice Sheet and the Liverpool Land coastal ice cap during the last two glacial cycles. *Journal of Quaternary Science* 20, 269–283.
- Balco, G., Stone, J. O., Lifton, N. A. & Dunai, T. J. 2008: A complete and easily accessible means of calculating surface exposure ages or erosion rates from ^{10}Be and ^{26}Al measurements. *Quaternary Geochronology* 3, 174–195.
- Bennike, O. & Böcher, J. 1994: Land biotas of the last interglacial/glacial cycle on Jameson Land, East Greenland. *Boreas* 23, 479–487.
- Biernan, P. R., Marsella, K. A., Patterson, C., Davis, P. T. & Caffee, M. 1999: Mid-Pleistocene cosmogenic minimum-age limits for pre-Wisconsin glacial surfaces in southwestern Minnesota and southern Baffin Island: A multiple nuclide approach. *Geomorphology* 27, 25–39.

- Björck, S. & Hjort, C. 1984: A re-evaluated glacial chronology for northern East Greenland. *Geologiska Föreningens i Stockholm Förhandlingar* 105, 235–243.
- Briner, J. P. 2003: *The Last Glaciation of the Clyde Region, Northeastern Baffin Island, Arctic Canada: Cosmogenic Isotopes Constraints on Laurentide Ice Sheet Dynamics and Chronology*. Ph.D. dissertation, University of Colorado, Boulder, 300 pp.
- Briner, J. P. 2007: Moraine pebbles and boulders yield indistinguishable ^{10}Be ages: A case study from Colorado, USA. *Eos Transactions AGU*, p. 88, Fall Meeting. Abstract PP33B-1272.
- Briner, J. P., Miller, G., Davies, P. T., Bierman, P. R. & Caffee, M. 2003: Last Glacial Maximum ice sheet dynamics in the Canadian Arctic inferred from young erratics perched on ancient tors. *Quaternary Science Reviews* 22, 437–444.
- Briner, J. P., Miller, G. H., Davis, T. R. & Finkel, R. 2005: Cosmogenic exposure dating in arctic glacial landscapes: Implications for the glacial history of northeastern Baffin Island, Arctic Canada. *Canadian Journal of Earth Sciences* 42, 67–84.
- Briner, J. P., Miller, G., Davies, P. T. & Finkel, R. 2006: Cosmogenic radionuclides from fiord landscapes support differential erosion by overriding ice sheets. *Geological Society of America Bulletin* 118, 406–430.
- Davis, P. T., Bierman, P. R., Marsella, K. A., Caffee, M. W. & Southon, J. R. 1999: Cosmogenic analysis of glacial terrains in the eastern Canadian Arctic: A test for inherited nuclides and the effectiveness of glacial erosion. *Annals of Glaciology* 28, 181–188.
- Davis, P. T., Briner, J. P., Coulthard, R. P., Finkel, R. W. & Miller, G. H. 2006: Preservation of Arctic landscapes overridden by cold-based ice sheets. *Quaternary Research* 65, 156–163.
- Dowdeswell, J. A., Uenzelmann-Neben, G., Whittington, R. J. & Marienfeld, P. 1994: The Late Quaternary sedimentary record in Scoresby Sund, East Greenland. *Boreas* 23, 294–310.
- Evans, J., Dowdeswell, J. A., Grobe, H., Niessen, F., Stein, R., Hubberten, H. W. & Whittington, R. J. 2002: Late Quaternary sedimentation in Kejsar Franz Joseph Fjord and the continental margin of East Greenland. In Dowdeswell, J. A. & O'Cofaigh, C. (eds.): *Glacier Influenced Sedimentation on High Latitude Continental Margins*, 149–179. Geological Society of London Special Publications 203.
- Fabel, D., Stroeven, A. P., Harbour, J., Kleman, J., Elmore, D. & Fink, D. 2002: Landscape preservation under Fennoscandian ice sheets determined from in situ produced ^{10}Be and ^{26}Al . *Earth and Planetary Science Letters* 201, 397–406.
- Funder, S. 1972: Remarks on the Quaternary geology of Jameson Land and adjacent areas, Scoresby Sund, East Greenland. *Grønlands Geologiske Undersøgelse Report* 48, 93–98.
- Funder, S. 1984: Chronology of the last interglacial/glacial cycle in Greenland: First approximation. In Mahaney, W. C. (ed.): *Correlation of Quaternary Chronologies*, 261–279. GeoBooks, Norwich.
- Funder, S. 1989: Quaternary geology of the ice-free areas and adjacent shelves of Greenland; Chapter 13. In Fulton, R. J. (ed.): *Quaternary Geology of Canada and Greenland*, 742–792. Geological Survey of Canada.
- Funder, S. 2004: Middle and late Quaternary glacial limits in Greenland. In Ehlers, J. & Gibbard, P. L. (eds.): *Quaternary Glaciations – Extent and Chronology, Part II*, 425–430. Elsevier, Amsterdam.
- Funder, S. & Hansen, L. 1996: The Greenland Ice Sheet – a model for its culmination and decay during and after the last glacial maximum. *Bulletin of the Geological Society of Denmark* 42, 137–152.
- Funder, S. & Hjort, C. 1973: Aspects of the Weichselian chronology in central East Greenland. *Boreas* 2, 69–84.
- Funder, S., Hjort, C. & Landvik, J. Y. 1994: The last glacial cycle in East Greenland, an overview. *Boreas* 23, 283–293.
- Funder, S., Hjort, C., Landvik, J. Y., Nam, S.-I., Reeh, N. & Stein, R. 1998: History of a stable ice margin – East Greenland during the middle and upper Pleistocene. *Quaternary Science Reviews* 17, 77–123.
- Gosse, J. C. & Phillips, F. M. 2001: Terrestrial in-situ cosmogenic nuclides: Theory and application. *Quaternary Science Reviews* 20, 1275–1290.
- Håkansson, L. 2008: The Late Quaternary Glacial History of Northeast Greenland; cosmogenic isotope constraints on chronology and ice dynamics. *LUNDQUA thesis* 61, 70 pp.
- Håkansson, L., Briner, J. P., Alexanderson, H., Aldahan, A. & Poschnert, G. 2007: ^{10}Be ages from coastal northeast Greenland constrain the extent of the Greenland Ice Sheet during the Last Glacial Maximum. *Quaternary Science Reviews* 26, 2316–2321.
- Hansen, L., Funder, S., Murray, A. S. & Mejdal, S. 1999: Luminescence dating of the last Weichselian Glacier advance in East Greenland. *Quaternary Geochronology* 18, 179–190.
- Harbour, J., Stroeven, A. P., Fabel, D., Clarkhall, A., Kleman, J., Li, Y., Elmore, D. & Fink, D. 2006: Cosmogenic nuclide evidence for minimal erosion across two subglacial sliding boundaries of the late glacial Fennoscandian ice sheet. *Geomorphology* 75, 90–99.
- Helsingør, B., Lal, D., Jull, A. J. T., Kubik, P., Ivy-Ochs, S., Knie, K. & Nolte, E. 2002: Production of selected cosmogenic radionuclides by muons: 2. Capture by negative muons. *Earth and Planetary Research Letters* 200, 357–369.
- Hjort, C. 1979: Glaciation in northern East Greenland during the Late Weichselian and Early Flandrian. *Boreas* 8, 281–296.
- Hjort, C. 1981: A glacial chronology for northern East Greenland. *Boreas* 10, 259–274.
- Hjort, C. & Salvigsen, O. 1991: The channel and tor landscape in southeastern Jameson Land, East Greenland. *LUNDQUA Report* 33, 23–26.
- Johnsen, S. J., Clausen, H. B., Dansgaard, W., Gundestrup, N. S., Hansson, M., Jonsson, P., Steffensen, J. P. & Sveinbjörnsdóttir, A. E. 1992: A ‘deep’ ice core from East Greenland. *Meddelelser om Grönland, Geoscience* 29, 22 pp.
- Kaplan, M. R., Corrato, A., Hulton, N. R. J., Rabassa, J. O., Kubik, P. W. & Freeman, S. P. H. T. 2007: Cosmogenic nuclide measurements in southernmost South America and implications for landscape change. *Geomorphology* 87, 284–301.
- Kohl, C. P. & Nishiizumi, K. 1992: Chemical isolation of quartz for measurement of in-situ produced cosmogenic nuclides. *Geochimica et Cosmochimica Acta* 56, 3583–3587.
- Lal, D. 1991: Cosmic ray labeling of erosion surfaces: In-situ nuclide production rates and erosion models. *Earth and Planetary Science Letters* 104, 424–439.
- Landvik, J. Y., Brook, E. J., Gaultieri, L., Raisbeck, G., Salvigsen, O. & Yiou, F. 2003: Northwest Svalbard during the last glaciation: Ice-free areas existed. *Geology* 31, 905–908.
- Landvik, J. Y., Lyså, A., Funder, S. & Kelly, M. 1994: The Eemian and Weichselian stratigraphy of the Langlandselv area, Jameson Land East Greenland. *Boreas* 23, 412–423.
- Lasca, N. P. 1969: The surficial geology of Skeldal, Mesters Vig, north east Greenland. *Meddelelser om Grönland* 176, 56 pp.
- Lyså, A. & Landvik, J. Y. 1994: The lower Jyllandselv succession: Evidence for three Weichselian glacier advances over coastal Jameson Land, East Greenland. *Boreas* 23, 434–446.
- Marienfeld, P. 1991: Holozäne sedimentationsentwicklung im Scoresby Sund, Ost-Grönland. *Berichte zur Polarforschung* 96, 162 pp.
- Marquette, G. C., Gray, J. T., Gosse, J. C., Courchesne, F., Stockli, L., Macpherson, G. & Finkel, R. 2004: Felsenmeer persistence under non-erosive ice in the Torngat Mountains and Kaumajet Mountains, Quebec and Labrador, as determined by soil weathering and cosmogenic nuclide exposure dating. *Canadian Journal of Earth Sciences* 41, 19–38.
- Möller, P., Hjort, C., Adrielsson, L. & Salvigsen, O. 1994: Glacial history of interior Jameson Land, East Greenland. *Boreas* 23, 320–348.
- Nam, S.-I., Stein, R., Grobe, H. & Hubberten, H. 1995: Late Quaternary glacial/interglacial changes in sediment composition at the East Greenland continental margin and their paleoceanographic implications. *Marine Geology* 122, 243–262.
- Nishiizumi, K. 2004: Preparation of ^{26}Al AMS standards. *Nuclear Instruments and Methods in Physics Research B* 223–224, 388–392.
- Nishiizumi, K., Imamura, M., Caffee, M. W., Southon, J. R., Finkel, R. C. & McAninch, J. 2007: Absolute calibration of ^{10}Be AMS standards. *Nuclear Instruments and Methods in Physics Research B* 258, 403–413.
- Nordenskjöld, O. 1907: On the Geology and Physical Geography of East Greenland. *Meddelelser om Grönland* 28, 151–284.
- O'Cofaigh, C., Dowdeswell, J. A., Evans, J., Kenyon, N. H., Taylor, J., Mienert, J. & Wilken, M. 2004: Timing and significance of glacially influenced mass-wasting in the submarine channels of the Greenland Basin. *Marine Geology* 207, 39–54.

- Putkonen, J. & O'Neil, M. A. 2006: Quaternary degradation of unconsolidated landforms in the western North America. *Geomorphology* 75, 408–419.
- Putkonen, J. & Swanson, T. 2003: Accuracy of cosmogenic ages for moraines. *Quaternary Research* 59, 255–261.
- Ronnert, L. & Nyborg, M. R. 1994: The distribution of different glacial landscapes on southern Jameson Land, East Greenland according to Landsat Thematic Mapper data. *Boreas* 23, 294–311.
- Schunke, E. 1986: Periglazialformen und Morphodynamik im südlichen Jameson Land, Øst-Grønland. *Abhandlungen der Akademie der Wissenschaften in Göttingen*, 142 pp.
- Stein, R., Grobe, H., Huberten, H., Marienfeld, P. & Nam, S. 1993: Latest Pleistocene to Holocene changes in glaciomarine sedimentation in Scoresby Sund and along the adjacent East Greenland continental margin: Preliminary results. *Geo-Marine Letters* 13, 9–16.
- Stein, R., Nam, S.-I., Grobe, H. & Huberten, H. 1996: Late Quaternary glacial history and short-term ice rafted debris fluctuations along the east Greenland continental margin. In Andrews (ed.): *Late Quaternary Paleoceanography of the North Atlantic Margins*, Geological Society Special Publication 111, 135–151.
- Stone, J. O. 2000: Air pressure and cosmogenic isotope production. *Journal of Geophysical Research* 105, 23753–23759.
- Stroeven, A. P., Fabel, D., Hätteström, C. & Harbour, J. 2002: A relict landscape in the centre of the Fennoscandian glaciation: Cosmogenic radionuclide evidence of tors preserved through multiple glacial cycles. *Geomorphology* 44, 145–154.
- Sugden, D. E. 1974: Landscapes of glacial erosion in Greenland and their relationship to ice, topographic and bedrock conditions. *Institute of British Geographers, Special Publication* 7, 177–195.
- Tveranger, T., Houmark-Nielsen, M., Løvberg, K. & Mangerud, J. 1994: Eemian – Weichselian stratigraphy of the Flakkerhuk ridge, southern Jameson land, East Greenland. *Boreas* 23, 359–384.
- Washburn, A. L. 1965: Geomorphic and vegetational studies in the Mesters Vig district. *Meddelelser om Grønland* 166, 60 pp.
- Wilken, M. & Mienert, W. 2006: Submarine glaciogenic debris-flows, deep-sea channel and past ice stream behaviour of the east Greenland continental margin. *Quaternary Science Reviews* 25, 784–810.